RESEARCH ARTICLES

STRUCTURAL BIOLOGY

Structural basis for chemokine recognition and activation of a viral G protein–coupled receptor

John S. Burg,[1,2,3] Jessica R. Ingram,[4] A. J. Venkatakrishnan,[3,5,6] Kevin M. Jude,[1,2,3] Abhiram Dukkipati,[1,2,3] Evan N. Feinberg,[3,5,6] Alessandro Angelini,[7] Deepa Waghray,[1,2,3] Ron O. Dror,[3,5,6] Hidde L. Ploegh,[4] K. Christopher Garcia[1,2,3]*

Chemokines are small proteins that function as immune modulators through activation of chemokine G protein–coupled receptors (GPCRs). Several viruses also encode chemokines and chemokine receptors to subvert the host immune response. How protein ligands activate GPCRs remains unknown. We report the crystal structure at 2.9 angstrom resolution of the human cytomegalovirus GPCR US28 in complex with the chemokine domain of human CX3CL1 (fractalkine). The globular body of CX3CL1 is perched on top of the US28 extracellular vestibule, whereas its amino terminus projects into the central core of US28. The transmembrane helices of US28 adopt an active-state–like conformation. Atomic-level simulations suggest that the agonist-independent activity of US28 may be due to an amino acid network evolved in the viral GPCR to destabilize the receptor's inactive state.

G protein–coupled receptors (GPCRs) engage a wide range of ligands, from small molecules to large proteins. The structures of GPCR complexes with small molecules and peptides have taught us much about recognition and activation mechanisms, including those of two human chemokine receptors bound to small molecules (1–4). However, proteins represent a substantial fraction of GPCR ligands for which there is currently a dearth of structural information.

Chemokines are protein GPCR ligands that function in immune modulation, wound healing, inflammation, and host-pathogen interactions, primarily by directing migration of leukocytes to inflamed or infected tissues (5, 6). One strategy that viruses use to evade the host immune response is to hijack mammalian chemokine GPCRs (7). Human cytomegalovirus (HCMV) encodes US28, a class A GPCR with 38% sequence identity to human CX3CR1 (8). An unusually promiscuous receptor, US28 binds chemokines from different families including CX3CL1 (fractalkine), which is tethered to endothelial cell membranes through an extended stalk (9).

Here we present two crystal structures of US28 in complex with the chemokine domain of human CX3CL1. Both structures (one bound to an alpaca nanobody at a resolution of 2.9 Å and the other without a nanobody at 3.8 Å) reveal a paradigm for chemokine binding that is applicable to chemokine-GPCR interactions more generally. Furthermore, the structure of US28 in both crystal forms suggests that this viral GPCR has evolved a highly stable active state to achieve efficient agonist-independent constitutive signaling.

Overall structure of the US28-CX3CL1 complex

The structure of US28 bound to the 77-amino acid chemokine domain of CX3CL1 is essentially identical with (Fig. 1A) and without (Fig. 1B) bound nanobody 7 (Nb7), with a carbon-α root mean square deviation (RMSD) of 0.42 Å. Nb7, which was selected from an immunized alpaca cDNA library (fig. S1), binds to the intracellular surface of US28 by projecting its three CDR loops into a central cavity between the transmembrane (TM) helices (fig. S2). The only major difference between these US28 structures is the orientation of helix 8, which runs parallel to the membrane in the nanobody-bound structure. In the nanobody-free structure, crystal packing prevents helix 8 from assuming this orientation (fig. S3).

The body of CX3CL1 sits perched above the extracellular US28 vestibule, whereas its N terminus projects deeply into the central cavity of US28 and occupies the ligand binding pocket, burying a surface area of ~1600 Å² (Fig. 1, A and B, and table S1). US28 accommodates this protein ligand by using its extracellular loops as "landing pads" upon which CX3CL1 sits. The CX3CL1 C terminus, truncated before the membrane-anchoring stalk, projects away from the complex. The globular body of CX3CL1 is less tightly constrained than its N-terminal peptide. Comparison of the two structures shows an ~2 Å wobble of CX3CL1 between the two crystal forms (fig. S4A), which may be rationalized by differences in crystal packing (fig. S4B).

Engagement of a chemokine by US28

In the structure of the US28-CX3CL1 complex, the globular chemokine body interacts with the receptor N terminus and extracellular loops (ECLs) (site 1), whereas the chemokine N terminus enters the helical core of the receptor (site 2), in accord with a two-site model (10). Site 1 is occupied by the bulkiest region of CX3CL1, with its C-terminal α helix completely outside the extracellular vestibule of the receptor (Fig. 2A). In site 2, the N-terminal peptide of CX3CL1 (residues 1 to 7) reaches to the bottom of the extracellular cavity, occupying the site that accommodates small molecules in many GPCR structures (Fig. 2A).

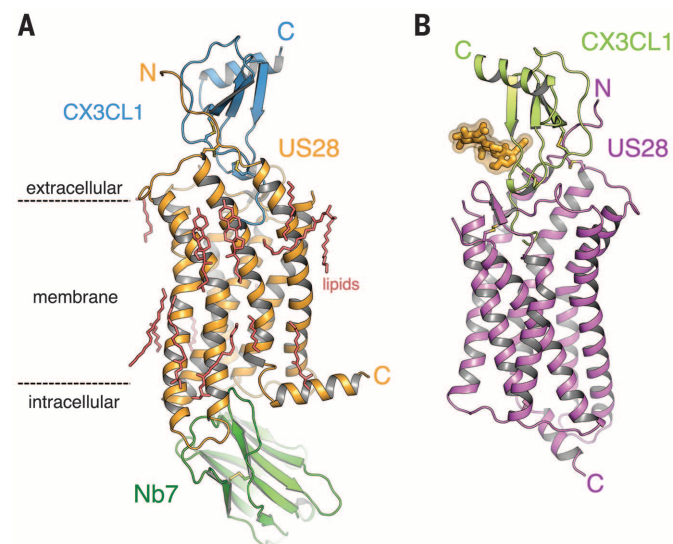The site 1 interaction accounts for most of the contact between US28 and CX3CL1, burying ~775 Å²

[1]Howard Hughes Medical Institute, Stanford University School of Medicine, Stanford, CA 94305, USA. [2]Department of Structural Biology, Stanford University School of Medicine, Stanford, CA 94305, USA. [3]Department of Molecular and Cellular Physiology, Stanford University School of Medicine, Stanford, CA 94305, USA. [4]Whitehead Institute for Biomedical Research, 9 Cambridge Center, Cambridge, MA 02142, USA. [5]Department of Computer Science, Stanford University, Stanford, CA 94305, USA. [6]Institute for Computational and Mathematical Engineering, Stanford University, Stanford, CA 94305, USA. [7]Koch Institute for Integrative Cancer Research, Massachusetts Institute of Technology, Cambridge, MA 02139, USA.
*Corresponding author. E-mail: kcgarcia@stanford.edu

Fig. 1. Structure of US28 in complex with CX3CL1. (**A**) Ternary complex of CX3CL1 (blue), US28 (orange), and nanobody (green) at 2.9 Å. (**B**) Binary complex of US28 (magenta) bound to CX3CL1 (light green). Asn-linked glycans are shown in yellow. C, C terminus; N, N terminus.

with 13 hydrogen bonds and 44 van der Waals interactions (Fig. 2, B and C, fig. S5, and table S1). The principal feature of site 1 is the N terminus of US28 winding along an extended groove on the surface of CX3CL1 formed in the junction between the β sheet and the N loop (Fig. 2, B and C). A similar binding cleft is apparent in the structures of several other chemokines (fig. S6) (11). The disulfide bond from receptor Cys23 to the third extracellular loop aligns the receptor's N terminus with the chemokine's binding cleft. The preceding US28 residue, Pro22, introduces a kink in the receptor N-terminal peptide that enhances its shape complementarity to the chemokine. Contacts between the US28 N terminus and CX3CL1 involve some side chains but are primarily interactions between their peptide backbones (Fig. 2C and table S1). The extensive main-chain contacts may enhance the ligand cross-reactivity of US28. Another important site 1 contact exists between a short mini-helix of CX3CL1 and ECL2 of US28 (Fig. 2D).

Tyr16 is the second US28 N-terminal residue modeled into electron density (fig. S7B), and corresponds to the position of a sulfated tyrosine found in some chemokine receptors, although it

is unclear whether US28 Tyr16 is sulfated. Many chemokines, including CX3CL1, contain strongly basic patches that are proposed to interact with sulfotyrosine in GPCR N-termini (fig. S6) (12, 13). However, Tyr16 is poorly ordered in US28 and does not appear to make specific contacts with CX3CL1.

As with other chemokines, the CX3CL1 N terminus was found to be highly flexible in previous structural studies (14). In contrast, we find that the N terminus of receptor-bound CX3CL1 is well ordered, extending to the bottom of the US28 ligand binding pocket and burying 623 Å^2 of surface area (Fig. 3A and fig. S7C). Residues 1 to 4 form a hooklike conformation at the base of the pocket, with residues 5 to 7 extending outward to link the N-terminal "hook" to the globular core of CX3CL1. CX3CL1 residue Gln1 is cyclized to form pyroglutamate (pGlu1) (Fig. 3, A and B), which is apparent both in the electron density map and by mass spectrometry (figs. S7C and S8). The CX3CL1 N-terminal hook contacts residues on TM1, TM3, TM7, and ECL2, with Tyr40$^{1.39}$, Tyr112$^{3.33}$, Thr175^{ECL2}, and Glu277$^{7.39}$ of US28 participating in hydrogen bonds with pGlu1, His2, His3, and Gly4 of CX3CL1 (Fig. 3, A and B) [superscripts refer to Ballesteros-

Weinstein nomenclature (15)]. Glu277$^{7.39}$ may also form a salt bridge with CX3CL1 His3. The extensive interactions of Glu277$^{7.39}$ with CX3CL1 provide a structural basis for the observation that Glu$^{7.39}$ is important for chemokine receptor signaling (16).

Comparison of the CX3CL1 binding mode with CXCR4 and CCR5 inhibitors

Human chemokine receptor structures have been previously reported as complexes with small-molecule (CCR5-maraviroc, CXCR4-IT1t) and peptide (CXCR4-CVX15) antagonists (2, 3). The overall helical structure of US28 superimposes closely with these structures (1.7 and 2.3 Å RMSD for CCR5 and CXCR4, respectively) (Fig. 4A). In the ligand binding pocket, maraviroc stretches across CCR5 from TM1 to TM5, whereas CX3CL1 occupies a smaller region of the ligand binding pocket concentrated toward TM1, TM2, TM3, and TM7 (Fig. 4B). The bonding chemistry of the maraviroc-CCR5 interaction grossly mimics the binding mode of CX3CL1 to US28, with the tropane and carboxamide nitrogens of maraviroc substituting for the His3 backbone amide and the His2 tau nitrogen of CX3CL1. The compact structure of CX3CL1's N-terminal hook suggests a potential pharmacophore that could be mimicked by small molecules. Several small-molecule inhibitors of US28 signaling have been developed (17, 18). One of these, VUF2274, is a four-ring structure with strong benzhydryl character that could conceivably mimic the N-terminal hook peptide of CX3CL1. The structure of CXCR4 bound to the cyclic peptide CVX15 also presents an instructive comparison with US28-CX3CL1 (3). Like CX3CL1, CVX15 fills almost the entire extracellular vestibule of its receptor and makes multiple contacts with ECL2 but leans toward the opposite side of the receptor vestibule near TM4, TM5, and TM6 (Fig. 4B, right panel).

US28 TM conformations and implications for the active state

US28 has been shown to exhibit agonist-independent activity, with CX3CL1 reportedly diminishing signaling as an inverse agonist (19). We find that both the nanobody-bound and -free US28-CX3CL1 complexes bear the structural hallmarks of an active state, as seen in previous structures (20). Nb7 appears to recognize a preformed active-state conformation of US28 present in the nanobody-free US28-CX3CL1 complex. This finding suggests that the CX3CL1-bound form of US28 is indeed active, although it may occupy an activation state distinct from unliganded US28.

The conformation of TM6 in US28 is typical of an active-state GPCR (20). Compared with the inactive-state CXCR4 and CCR5 structures, US28 exhibits an outward movement (~9 Å) at the intracellular end of TM6 (Fig. 5A). Other conserved structural motifs also display signatures of receptor activation (20). These include the DRY motif (Asp128$^{3.49}$, Arg129$^{3.50}$, and Tyr130$^{3.51}$) located at the intracellular side of TM3 and the NPXXY motif (Asn287$^{7.49}$, Pro288$^{7.50}$, and Tyr291$^{7.53}$) in TM7. US28 Arg129$^{3.50}$ of the DRY motif extends
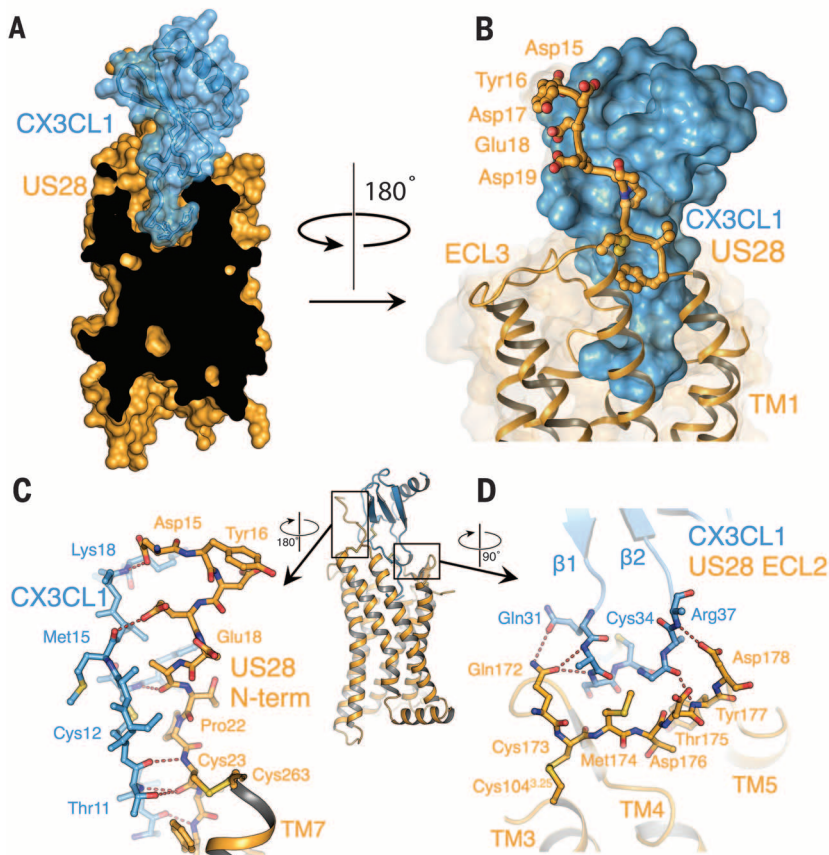

Fig. 2. Interaction of the US28 N terminus with CX3CL1 (site 1). (**A**) Cutaway surface representation of CX3CL1 (blue) bound to US28 (orange). (**B**) The N-terminal region of US28 forms a large contact surface with CX3CL1. Side chains of US28 interacting with CX3CL1 are shown as sticks. (**C**) Amino acid interactions between CX3CL1 and US28 at chemokine binding site 1. The entire US28-CX3CL1 complex is shown for reference with the nanobody removed for clarity. (**D**) Amino acid interactions between US28 ECL2 and the β1-β2 loop of fractalkine.

inward toward the center of the TM bundle, similar to the position seen in the active-state structure of the β2-adrenergic receptor (β2AR) and contrasting with the corresponding arginine in the inactive CCR5 structure that projects away (Fig. 5C) (2, 21). The DRY motif can stabilize the inactive conformation of some GPCRs by participating in a salt bridge between Arg$^{3.50}$ and an acidic residue at position 6.30, in what is known as the "ionic lock" (20, 22). US28 lacks an acidic residue at position 6.30, so absence of this contact could be one factor contributing to stabilization of the active state in the absence of ligand.

Further structural evidence for the active state of US28 is demonstrated by the intracellular half of TM7, which is shifted toward the center of the TM bundle (Fig. 5A). This is seen in the active-state β2AR but not the inactive CCR5 structure (2, 21). The inward movement of TM7 results in Tyr291$^{7.53}$ of the NPXXY motif shifting 7 Å toward the center of the TM bundle, which is close enough to TM5 and TM3 to form hydrogen bonds with Tyr208$^{5.58}$ and Ile122$^{3.43}$ through a water molecule (Fig. 5B). Tyr208$^{5.58}$, in turn, forms a hydrogen bond with Arg129$^{3.50}$ of the DRY motif

(Fig. 5C). This completes a hydrogen bond network connecting TM3, TM5, and TM7 that has been seen in previously solved active-state structures (20, 21).

CX3CL1 has been shown to exhibit both agonist and inverse agonist activities in US28 signaling assays. This apparent discrepancy has been explained by CX3CL1 being a "camouflaged agonist" that signals but exhibits diminished agonist activity due to ligand-induced internalization and degradation (23). These structures support an interpretation that CX3CL1 is an agonist, not an inverse agonist, because it does not induce an inactive state of the receptor. CX3CL1 binding may either stabilize the ligand-independent active state of US28 or alter the active conformation to induce a slightly different signaling outcome from the unliganded state.

Structural basis for constitutive activity and ligand action

Constitutive activity is a common property of viral GPCRs that enhances viral pathogenesis (18) and is also seen to varying degrees in some mammalian GPCRs (24, 25). Although structures of

certain constitutively active rhodopsin mutants are available (26, 27), the mechanistic basis through which viral GPCRs have gained this evolutionarily advantageous constitutive activity has remained unclear.

To address this question, we performed atomic-level molecular dynamics (MD) simulations of US28, both with and without bound CX3CL1 (see supplementary materials and methods). Atomic-level simulations have provided mechanistic insight into important functional properties of other GPCRs (28, 29). Because the crystal structures of US28 with and without the nanobody exhibit essentially identical conformations of the TM helices, we initiated our simulations from the 2.9 Å structure but omitted the nanobody.

Using integrated analysis of sequence, structure, and simulations of US28, we uncovered molecular features of US28 that may lead to its constitutive activity. In particular, we found that US28 has evolved a distinctive structure environment around Asp128$^{3.49}$, near the cytoplasmic end of TM3, that probably results in a destabilization of the receptor's inactive state (Fig. 6). Asp$^{3.49}$ is part of the conserved DRY motif, which
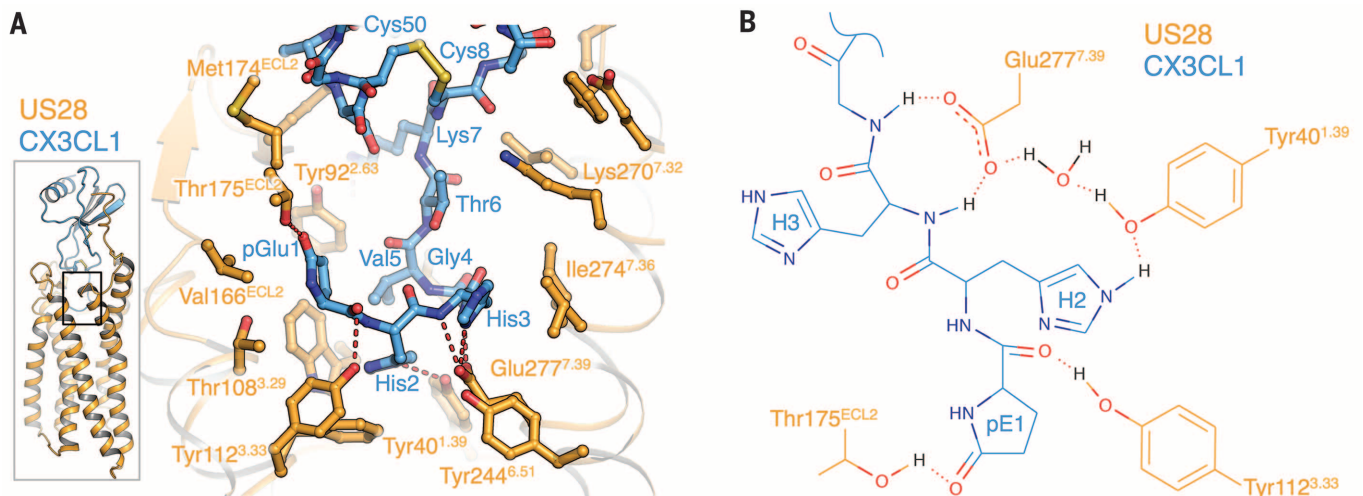

Fig. 3. Interaction of the CX3CL1 N terminus with the US28 ligand binding pocket (site 2). (**A**) Side chain contacts between CX3CL1 site 2 region (blue) and US28 (orange). (**B**) Two-dimensional plot of side-chain contacts between the CX3CL1 N-terminal hook and US28.
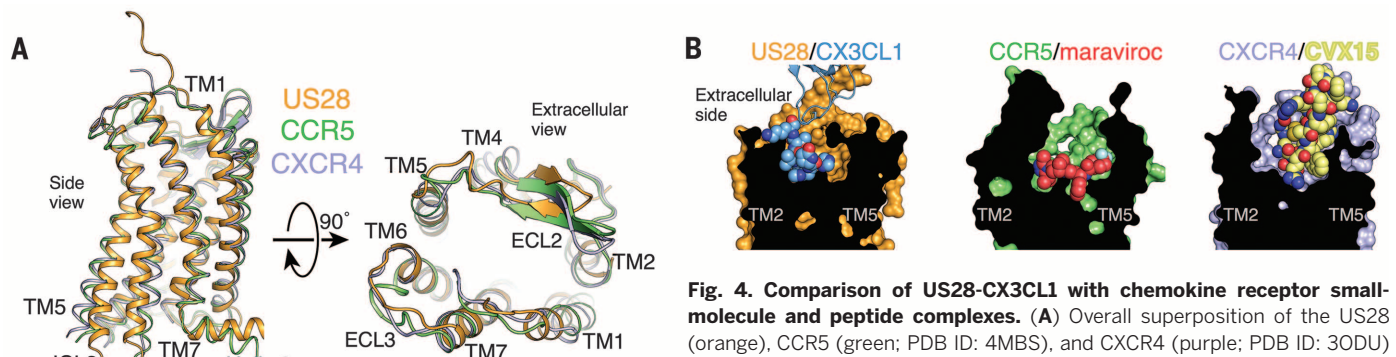

Fig. 4. Comparison of US28-CX3CL1 with chemokine receptor small-molecule and peptide complexes. (**A**) Overall superposition of the US28 (orange), CCR5 (green; PDB ID: 4MBS), and CXCR4 (purple; PDB ID: 3ODU) TM helices from the side (left) and as viewed from extracellular space (right). (**B**) Surface cutaway side views comparing ligand binding modes for US28-CX3CL1 (orange-blue), CCR5-maraviroc (green-red; PDB ID: 4MBS), and CXCR4-CVX15 (purple-yellow; PDB ID: 3OEO).
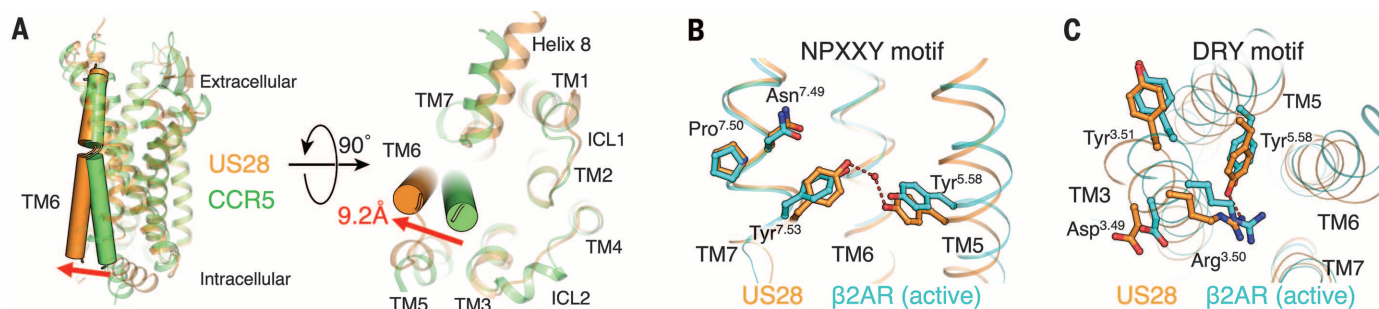
Fig. 5. Active-state hallmarks of US28 bound to CX3CL1. (**A**) Comparison between the TM6 conformations of US28 (orange) and CCR5 (green; PDB ID: 4MBS). (**B**) The NPXXY motif of US28 (orange) forms side-chain contacts resembling the active-state conformation of β_2AR (light blue; PDB ID: 3SN6). (**C**) The DRY motif of US28 (orange) forms side-chain contacts resembling the active-state conformation of β_2AR (light blue).
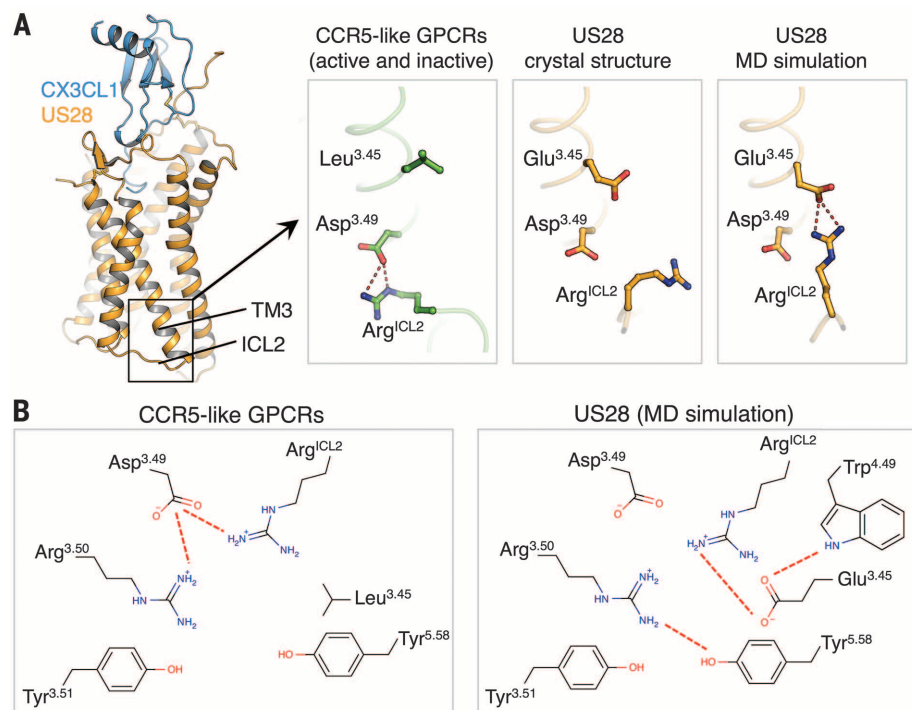

Fig. 6. Structural basis for the constitutive activity of US28. (**A**) Conformations of Arg$^{\text{ICL2}}$ in CCR5 (green; PDB ID: 4MBS; left), the US28 crystal structure (orange; center) and the US28 MD simulations (orange; right). (**B**) Schematic diagram of the network of side-chain interactions surrounding the DRY motif in CCR5 (left panel) and US28 (MD simulation; right).

plays an important role in the conformational transition between active and inactive states of class A GPCRs (*20*). An ionic interaction between Asp$^{3.49}$ and the neighboring Arg$^{3.50}$ generally stabilizes the inactive state of these receptors and is broken upon G protein coupling (Fig. 5C).

In many previously published GPCR structures, including all those of chemokine receptors, Asp$^{3.49}$ engages in a polar interaction with another arginine residue separate from the DRY motif on the second intracellular loop (ICL2); this arginine residue points toward the interior of the TM helical bundle (Fig. 6A, left panel). Mutation of this arginine has been associated with constitutive activity (*30*), suggesting that this residue is important for stabilizing the inactive state. In the US28 crystal structure, the

corresponding arginine, Arg139$^{\text{ICL2}}$, is pointing outward, probably as a result of the crystal lattice contacts it forms (Fig. 6A and fig. S9).

In MD simulations of US28 embedded in a lipid bilayer, Arg139$^{\text{ICL2}}$ immediately reorients toward the center of the bundle and assumes its most favored rotamer, but instead of contacting Asp128$^{3.49}$, it forms an ionic interaction with Glu124$^{3.45}$ (Fig. 6 and fig. S9B). This glutamate residue appears to function as an "ionic hook" that pulls Arg139$^{\text{ICL2}}$ upward, preventing it from interacting with Asp128$^{3.49}$ and, thus, potentially destabilizing the inactive state of the receptor (Fig. 6). Notably, the presence of a glutamate residue at position 3.45 is exclusive to the viral GPCR US28; it is not observed in any human class A GPCR. Together, these changes create

a different constellation of interactions centered on the DRY motif that favors the formation and stabilization of an active conformation.

Several other distinctive features of US28 may also contribute to the environment of Asp128$^{3.49}$ and destabilization of the inactive state. First, the ionic hook Glu124$^{3.45}$ is held in place by a hydrogen bond to Trp151$^{4.49}$ (Fig. 6B, right panel). Like Glu124$^{3.45}$, the tryptophan residue at this position is also absent from all human class A GPCRs. Second, ICL2 is shorter by four residues in US28 than in most class A GPCRs, which appears to prevent the formation of an α helix in ICL2. When such an α helix does form in other GPCRs, it appropriately positions the ICL2 arginine to interact with Asp$^{3.49}$, so the lack of ICL2 secondary structure in US28 may be providing Arg139$^{\text{ICL2}}$ the flexibility required to adopt different structural states. Finally, in most other class A GPCR structures, including those of chemokine receptors, Asp$^{3.49}$ engages in a hydrogen bond with the residue at position 2.39 in TM2. In US28, this residue is replaced by a glycine, which is incapable of forming such an interaction, while a serine introduced at the neighboring position 2.38 engages in a hydrogen bond with Asp128$^{3.49}$; this shift appears to alter the side-chain conformation of Asp128$^{3.49}$.

Other viral GPCR systems might have adopted a similar strategy to achieve constitutive activity. In US27 from HCMV, the position equivalent to the US28 ionic hook Glu$^{3.45}$ is an asparagine residue, which is also absent from human class A GPCRs. In the Kaposi's sarcoma–associated herpesvirus GPCR ORF74, Asp$^{3.49}$ is mutated to Val$^{3.49}$, preventing any ionic interaction with Arg$^{3.50}$. Molecular tinkering with the GPCR regions important for conformational switching, such as the DRY motif and its immediate environment, may thus represent a common evolutionary strategy in viruses to achieve constitutive activity and enhance viral pathogenesis.

Summary

The structure of the human CX3CL1 chemokine domain bound to HCMV US28 serves as a model for other mammalian and viral chemokine GPCR-ligand complexes. The viral origins of US28 have allowed us to gain insight into the evolutionary strategies that viruses use to tune GPCR signaling

properties to promote their survival and propagation. Furthermore, these viral-derived structural insights shed light on the mechanisms of ligand signal-tuning and constitutive activity of mammalian GPCRs as a whole. The tunability of US28, and perhaps other viral GPCRs, suggests that chemokine ligand-engineering strategies to elicit differential and biased signaling from GPCRs may be a productive way to create new agonistic and inhibitory ligands.

REFERENCES AND NOTES

1. V. Katritch, V. Cherezov, R. C. Stevens, *Annu. Rev. Pharmacol. Toxicol.* **53**, 531–556 (2013).
2. Q. Tan *et al.*, *Science* **341**, 1387–1390 (2013).
3. B. Wu *et al.*, *Science* **330**, 1066–1071 (2010).
4. D. M. Rosenbaum, S. G. Rasmussen, B. K. Kobilka, *Nature* **459**, 356–363 (2009).
5. I. F. Charo, R. M. Ransohoff, *N. Engl. J. Med.* **354**, 610–621 (2006).
6. A. E. Proudfoot, *Nat. Rev. Immunol.* **2**, 106–115 (2002).
7. A. Sodhi, S. Montaner, J. S. Gutkind, *Nat. Rev. Mol. Cell Biol.* **5**, 998–1012 (2004).
8. M. S. Chee, S. C. Satchwell, E. Preddie, K. M. Weston, B. G. Barrell, *Nature* **344**, 774–777 (1990).
9. J. F. Bazan *et al.*, *Nature* **385**, 640–644 (1997).
10. S. Thiele, M. M. Rosenkilde, *Curr. Med. Chem.* **21**, 3594–3614 (2014).
11. M. Szpakowska *et al.*, *Biochem. Pharmacol.* **84**, 1366–1380 (2012).
12. C. J. Millard *et al.*, *Structure* **22**, 1571–1581 (2014).
13. C. T. Veldkamp *et al.*, *Sci. Signal.* **1**, ra4 (2008).
14. L. S. Mizoue, J. F. Bazan, E. C. Johnson, T. M. Handel, *Biochemistry* **38**, 1402–1414 (1999).
15. J. A. Ballesteros, H. Weinstein, *Methods Neurosci.* **25**, 366–428 (1995).
16. A. Brelot, N. Heveker, M. Montes, M. Alizon, *J. Biol. Chem.* **275**, 23736–23744 (2000).
17. P. Casarosa *et al.*, *J. Biol. Chem.* **278**, 5172–5178 (2003).
18. H. F. Vischer, M. Siderius, R. Leurs, M. J. Smit, *Nat. Rev. Drug Discov.* **13**, 123–139 (2014).
19. H. F. Vischer, R. Leurs, M. J. Smit, *Trends Pharmacol. Sci.* **27**, 56–63 (2006).
20. A. J. Venkatakrishnan *et al.*, *Nature* **494**, 185–194 (2013).
21. S. G. Rasmussen *et al.*, *Nature* **477**, 549–555 (2011).
22. K. Palczewski *et al.*, *Science* **289**, 739–745 (2000).
23. M. Waldhoer *et al.*, *J. Biol. Chem.* **278**, 19473–19482 (2003).
24. C. T. Gilliland, C. L. Salanga, T. Kawamura, J. Trejo, T. M. Handel, *J. Biol. Chem.* **288**, 32194–32210 (2013).
25. X. Han, *Adv. Pharmacol.* **70**, 265–301 (2014).
26. X. Deupi *et al.*, *Proc. Natl. Acad. Sci. U.S.A.* **109**, 119–124 (2012).
27. J. Standfuss *et al.*, *Nature* **471**, 656–660 (2011).
28. R. O. Dror *et al.*, *Proc. Natl. Acad. Sci. U.S.A.* **108**, 18684–18689 (2011).
29. R. O. Dror *et al.*, *Nature* **503**, 295–299 (2013).
30. E. S. Burstein, T. A. Spalding, M. R. Brann, *J. Biol. Chem.* **273**, 24322–24327 (1998).

STRUCTURAL BIOLOGY

Crystal structure of the chemokine receptor CXCR4 in complex with a viral chemokine

Ling Qin,[1]* Irina Kufareva,[1]*† Lauren G. Holden,[1]* Chong Wang,[2] Yi Zheng,[1] Chunxia Zhao,[1] Gustavo Fenalti,[2] Huixian Wu,[2] Gye Won Han,[3,4] Vadim Cherezov,[3] Ruben Abagyan,[1] Raymond C. Stevens,[3,4]† Tracy M. Handel[1]†

Chemokines and their receptors control cell migration during development, immune system responses, and in numerous diseases, including inflammation and cancer. The structural basis of receptor:chemokine recognition has been a long-standing unanswered question due to the challenges of structure determination for membrane protein complexes. Here, we report the crystal structure of the chemokine receptor CXCR4 in complex with the viral chemokine antagonist vMIP-II at 3.1 angstrom resolution. The structure revealed a 1:1 stoichiometry and a more extensive binding interface than anticipated from the paradigmatic two-site model. The structure helped rationalize a large body of mutagenesis data and together with modeling provided insights into CXCR4 interactions with its endogenous ligand CXCL12, its ability to recognize diverse ligands, and the specificity of CC and CXC receptors for their respective chemokines.

The chemokine receptor CXCR4 controls cell migration during immune surveillance and development of the cardiovascular, hematopoietic, and central nervous systems (*1–3*). Like many other chemokine receptors (CKRs), CXCR4 contributes to inflammatory diseases and cancer (*4*, *5*). It also functions as one of two co-receptors that facilitate entry of HIV into host immune cells (*6*). Despite the importance of CXCR4 and CKRs in general, structural insights into CKR: chemokine recognition have been limited to nuclear magnetic resonance studies of chemokines with peptides derived from CKR N termini (*7–9*). This is partly due to the challenges of structure determination for full-length membrane proteins and their complexes.

Here, we present the structure of CXCR4 in complex with vMIP-II, a CC chemokine encoded by Kaposi's sarcoma–associated herpesvirus. vMIP-II functions as a broad-spectrum antagonist of many human CKRs (*10*) and helps the virus to escape the host immune response (*11*). We chose vMIP-II for structural studies because it is a high-affinity antagonist of CXCR4 [median inhibitory concentration, 6 to 15 nM (*10*, *12*)] and, as a ligand for both CC and CXC chemokine receptors, was expected to provide insight into ligand recognition specificity.

Design of an irreversible CXCR4:vMIP-II complex

Despite high affinity in membranes, the CXCR4: vMIP-II complex was insufficiently stable in de-

[1]University of California, San Diego, Skaggs School of Pharmacy and Pharmaceutical Sciences, La Jolla, CA 92093, USA. [2]Department of Integrative Structural and Computational Biology, The Scripps Research Institute, 10550 North Torrey Pines Road, La Jolla, CA 92037, USA. [3]Department of Chemistry, Bridge Institute. [4]Department of Biological Sciences, Bridge Institute, University of Southern California, Los Angeles, CA 90089, USA.
*These authors contributed equally to this work. †Corresponding author. E-mail: thandel@ucsd.edu (T.M.H.); stevens@usc.edu (R.C.S.); ikufareva@ucsd.edu (I.K.)

tergent to justify crystallization trials. We therefore employed a strategy that uses disulfide trapping to generate an irreversible complex (*13*, *14*). Co-expression of pairs of single cysteine mutants of CXCR4 and vMIP-II was expected to result in spontaneous formation of a disulfide bond if the disulfide was compatible with the native geometry of the CKR:chemokine complex. Guided by three-dimensional models of CXCR4:chemokine complexes (*14*), 37 cysteine mutant pairs were designed, and, for each pair, the abundance of disulfide-trapped complexes was evaluated (*15*). These pairs included seven N-terminal cysteine mutants of vMIP-II that were systematically coexpressed with two CXCR4 cysteine mutants, $D97^{2.63}C$ or $D187^{ECL2}C$ [superscript denotes the Ballesteros-Weinstein index (*16*, *17*) for helical domain residues; ECL is extracellular loop]. Of all mutant pairs analyzed, CXCR4(D187C) coexpressed with vMIP-II(W5C) formed the highest percentage of trapped complex (Fig. 1A). It also showed an unfolding temperature of 63°C (Fig. 1B), which is 4° to 14°C higher than other mutant combinations, and excellent monodispersity when analyzed by size-exclusion chromatography (fig. S1). By comparison, the mutant pair with the second highest melting temperature, CXCR4(D187C): vMIP-II(H6C) (59°C), was produced in significantly lower yield and showed lower monodispersity, despite the adjacent position of the vMIP-II cysteine (fig. S1). CXCR4(D97C) formed little or no covalent complex with any of the seven vMIP-II mutants tested (Fig. 1, A and B). The observed sensitivity of several biophysical properties of the complex to precise cysteine placement suggests specificity of the disulfide-trapping approach and supports compatibility of the D187C:W5C disulfide bond with the native complex geometry. We therefore selected CXCR4(D187C):vMIP-II(W5C) for crystallization in lipidic cubic phase (LCP) (*18*) and determined the structure at 3.1 Å resolution. Data